J. S. Afr. Inst. Min. Metall., vol. 89, no. 8.
Jul. 1989. pp. 193-200.

The influence on galvanic corrosion tests of resistance in the metallic conduction path

by P.C. PISTORIUS* and R.F. SANDENBERGH*

SYNOPSIS

By use of a finite-difference model of an experimental galvanic cell, the effect of a resistance in the metallic conduction path on the potential and current distributions in the cell was predicted. The model predictions were compared with experimental measurements of potential profiles (measured by use of a scanning reference electrode) and galvanic currents. The predictions agreed well with the experimental measurements. Apart from this model, which is applicable in macroscopic cells (i.e. with an electrolyte of low conductivity), a calculation procedure was developed to predict the effect of an external resistance on the galvanic current in a microscopic cell (high conductivity). The responses of the galvanic currents in the microscopic and macroscopic cells to changes in the external resistance were compared. From the similarity of the responses, a simple practical procedure for the evaluation of the external resistance (meter resistance) that can be tolerated is proposed.

SAMEVATTING

Die uitwerking van 'n weerstand in die metaalgeleidingsbaan op die potensiaal- en stroomverdelings in die sel is voorspel met gebruik van 'n meetbareverskilmodel van 'n eksperimentele galvaniese sel. Die modelvoorspellings is vergelyk met eksperimentele metings van potensiaalprofiele (gemeet met gebruik van 'n aftasverwysingselektrode) en galvaniese strome. Die voorspellings het goed met die eksperimentele metings ooreengekom. Benewens hierdie model, wat van toepassing is in makroskopiese selle (d.w.s. met 'n elektroliet met 'n lae geleivermoë) is daar 'n berekeningsprosedure ontwikkel om die uitwerking van 'n uitwendige weerstand op die galvaniese stroom in 'n mikroskopiese sel (hoë geleivermoë) te voorspel. Die responsies van die galvaniese strome in mikroskopiese en makroskopiese selle op veranderinge in die uitwendige weerstand, is vergelyk. Aan die hand van die ooreenkoms tussen die responsies, word daar 'n eenvoudige praktiese prosedure vir die evaluering van die uitwendige weerstand (meterweerstand) wat toegelaat kan word, aan die hand gedoen.

Introduction

Galvanic corrosion (or bimetallic corrosion) occurs when two dissimilar metals are connected electrically while exposed to a corrosive environment. Because of this contact, the more reactive metal generally corrodes at a higher rate than when uncoupled, while the less reactive (more noble) metal is generally protected by the contact. The more reactive metal acts as the anode in the couple, and the more noble metal as the cathode. The increased corrosion of the anode is caused by the galvanic current, which flows in the electrolyte from the anode to the cathode (and in the metallic conduction path from the cathode to the anode).

Galvanic corrosion is one of the most common forms of corrosion[1] and plays an important role in nearly every form of localized corrosion[2]. Owing to considerations of strength and economy, it is not always possible to avoid contact between dissimilar metals, for example in the construction of pumping equipment[3], and in aircraft and aerospace applications[1]. During welding, the filler metal may be different from the parent metal in the interests of mechanical properties. Composite materials, for example aluminium alloys alloyed with carbon fibre[4] and uranium alloys reinforced with tungsten fibre[5], may suffer severe localized attack where the fibres are exposed, for example by machining, with a resultant loss of strength. Couples between bare steel and reinforcing bar in concrete are not uncommon[6], in which case the bare steel serves as the anode. The detrimental effects of such a couple may include accelerated corrosion of the anode, and structural damage of the concrete due to altered chemistry or product accumulation[6].

Galvanic corrosion is utilized to good effect in atmospheric corrosion meters[7] and sacrificial cathodic protection systems[8].

Galvanic effects between electrically conductive minerals play an important role in the wet processing of ores and minerals. These effects accelerate or retard leaching, and may have a strong influence on the adsorption of collectors on the surface of minerals during flotation[9].

Localized corrosion is characterized by fixed anodic positions on the surface of the corroding metal, with the surrounding metal surface serving as the cathode. This is a case where a galvanic couple exists on the surface of a single metal. The development of localized electrodes is the result of differences in electrochemical activity, or a combination of geometric and electrochemical effects. For example, during pitting and crevice corrosion, the metal within the pit or crevice is anodic and remains so because of the autocatalytic effect of local acidification (and the accumulation of chlorides if present) within the pit or crevice[10].

Stainless steels become susceptible to intergranular corrosion when they are sensitized, which happens as a result of the precipitation of chromium carbides at the grain boundaries. These deplete the area of the grain close to the grain boundary of chromium, owing to the higher mobility of carbon (an interstitial) in the metal lattice

* Department of Materials Science and Metallurgical Engineering, University of Pretoria, 0002 Pretoria.

ISSN 0038-223X/$3.00 + 0.00. Paper received 3rd October, 1988.

relative to the mobility of chromium[10]. As stainless steels depend on their contained chromium for corrosion resistance, the depletion of chromium leads to a loss of corrosion resistance near the grain boundaries, causing a galvanic cell to develop between the depleted and the undepleted areas. This is the cause of intergranular corrosion.

Galvanic corrosion also plays a role during stress-corrosion cracking, for example of Al-Mg and Al-Cu alloys[11], and of AISI type 304 stainless steel[12].

These examples illustrate the importance of galvanic corrosion, and point to the need for an understanding of this effect.

Measuring the galvanic current between the anode and the cathode of a galvanic couple is an important way of studying galvanic corrosion. When the galvanic current that flows between the elements of a galvanic couple is measured, it is important that the current meter used does not disturb the galvanic-corrosion process. The meter can disturb the process if it places an unduly large resistance in the metallic (electronic) conduction path. For this reason, zero resistance ammeters (ZRAs) are normally used for the measurement of galvanic current. Potentiostatic[2], galvanostatic[2], and operational amplifier[13] ZRAs have been described.

In the construction of a potentiostatic ZRA, one of the electrodes of the galvanic couple is connected to the potentiostat as the working electrode, and the other electrode of the couple is connected to both the reference-electrode and the counter-electrode inputs of the potentiostat. The potentiostat is set to maintain a zero potential difference between the working electrode and the reference electrode (which is effectively the same as the short-circuiting of two electrodes of a galvanic couple). The current supplied by the potentiostat to maintain the zero potential difference is the galvanic or short-circuit current.

The typical accuracy of the set voltage of a potentiostat is 2 mV. In a previous investigation[14], the galvanic currents were typically of the order of 100 μA. If the potentiostat imposes a potential drop of 2 mV between the cathode and the anode of the couple, this is equivalent to a resistance of 20 Ω in the metallic conduction path.

The simplest method of measuring the galvanic current is to connect the anode and the cathode through a low, known resistance, and to measure the potential drop across this resistance[15]. This method was favoured previously, and is attractive if a computerized data-acquisition system is used because the galvanic currents of many couples can be monitored by measurement of the potential drops across the known resistances, using the multiple input ports of an analogue-to-digital converter. This method was used in a recent investigation[16], in which the galvanic current between electrodes of various metals (copper-nickel alloys, bronzes, steel, titanium, and zinc) in sea water was monitored by measurement of the potential drop across a resistance of 1 Ω. It was found that the addition of this resistance had only an insignificant effect on the behaviour of the couple.

From this discussion, it appears that the concept of zero resistance is somewhat unclear, and the finite-difference model described elsewhere[14] was used to investigate the possible use of such a model to predict the influence of an external resistance.

Experimental

The experimental setup is shown schematically in Fig. 1. Galvanic couples between carbon steel and AISI type 304 stainless steel were made up by the mounting of parallel strips of these metals in epoxy resin (with a 30 mm metallographic mount). The strips were ground to a 600 grit finish. Leads soldered to the backs of the strips provided electrical connections. The potential profiles across the galvanic couple were measured by the technique of the scanning reference electrode. This technique (SRET)[12] uses a micro-electrode placed close to the surface of the specimen (typically tens of micrometres away from the surface). The electrode is scanned across the surface to measure potential variations in the solution above the sample surface, e.g. to locate anodes and cathodes during localized corrosion and to study their development with time.

In this experimental setup, two stepping motors were used to move the sample relative to the micro-electrode, which was fixed. The stepping motors were controlled by a personal computer. The potential measurement at each position was read into the computer with an analogue-to-digital converter after the potential signal had been passed in sequence through a potentiostat and an amplifier. A potentiostat was used for the measurement of the potentials to provide the high input impedance necessitated by the high tip resistance of the micro-electrode. A tin-tin oxide electrode[17] with an outer diameter of 50 μm was used, with a tip resistance (polarization resistance) of the order of 10^9 Ω. The tin-tin oxide electrode was positioned 50 μm above the surface of the sample. To avoid screening effects, the electrode was not placed any closer to the surface.

As Fig. 1 illustrates, the strips could be short-circuited through a ZRA (a Keithley Model 614 Electrometer) so that the galvanic current flowing from the cathode to the anode could be measured, or the strips could be separated electrically. The latter condition was used when the polarization characteristics of the strips was determined separately. For the determination of the polarization characteristics, the tin-tin oxide electrode was used as a reference electrode. A counter electrode was made up from four 5 mm by 10 mm pieces of platinum foil (welded to platinum wire with capacitive discharge welding) and added to the SRET cell.

The galvanic couple was immersed in a solution with a conductivity of 98 mS/m. The electrolyte had a pH value of 3,0 and was made up from sulphuric acid, deionized water, and sodium sulphate. The electrolyte was aerated, and the test temperature was 18,1°C. The galvanic current between the cathode and the anode, as well as the potential profiles across the couple, were measured with resistances of various sizes in series with the ZRA shown in Fig. 1.

The galvanic cell considered here was a *macroscopic* cell, which means that the solution resistance was significant. In such a cell, the solution potential varies with position, being more positive near anode(s) than near cathode(s), and the distribution of the galvanic current on the electrodes is non-uniform. In a *microscopic* cell,

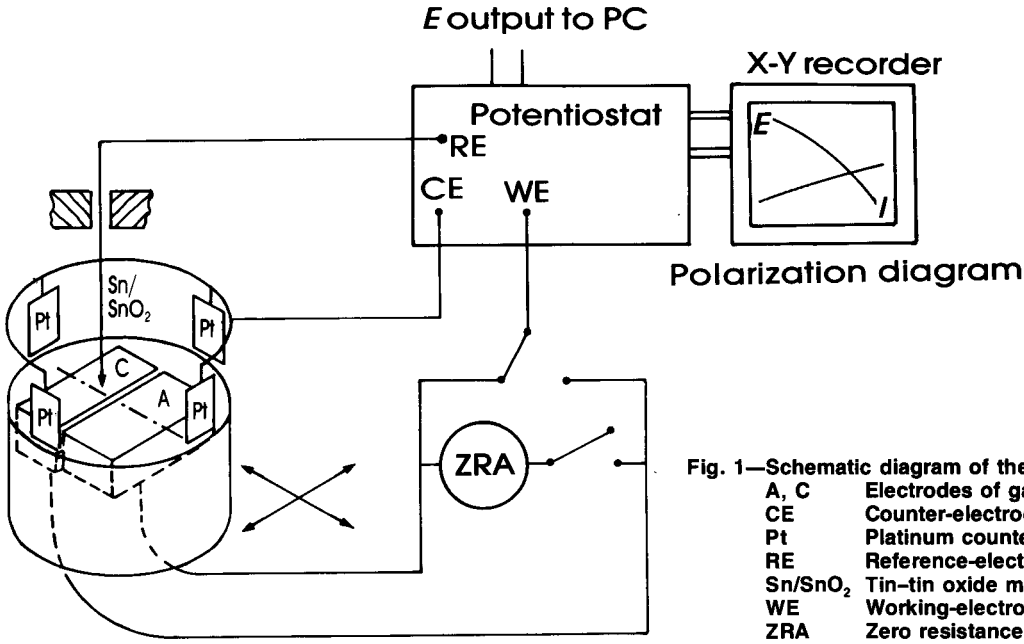

Fig. 1—Schematic diagram of the experimental setup

A, C	Electrodes of galvanic couple
CE	Counter-electrode connector
Pt	Platinum counter-electrode
RE	Reference-electrode input
Sn/SnO_2	Tin–tin oxide micro-electrode
WE	Working-electrode connector
ZRA	Zero resistance ammeter

the solution conductivity is so high that the solution resistance is negligible, with the result that the solution potential does not vary with position, and the distributions of current on the electrodes are uniform.

Whether a galvanic cell will behave macroscopically or microscopically is determined by the polarization resistances of the electrodes and the solution resistance. The polarization resistance involved here is the slope of the *size-dependent* polarization diagram (potential *vs* current). If the polarization resistance is much larger than the solution resistance, the distribution of current on the electrode is uniform and the potential variation in the solution near the galvanic couple is negligible. This is the microscopic case. If the polarization resistance of the electrode is much smaller than the solution resistance, the current distribution will be non-uniform and the solution potential will also vary with position (macroscopic case). The distinction between macroscopic and microscopic cells can be quantified by means of the Wagner parameter[18].

Modelling Approach

The finite-difference model of the galvanic cell and its validation have been described elsewhere[14]. The essential features of the model are illustrated in Fig. 2. The electrolyte is divided into rectangular elements on the assumption that each element has a constant solution potential, and a current balance is written for each element. The current balances yield a set of simultaneous equations for the solution potentials of the elements, and the equations are solved by means of the method of successive over-relaxation, which is an iterative method. The potentials of all the elements are recalculated by means of an iterative formula until the potential values change by less than a specified amount (the tolerance) after successive calculations (or iterations). Once the potentials have been calculated, the current density at any point in the electrolyte can be calculated from Ohm's law.

A small modification to the finite-difference model

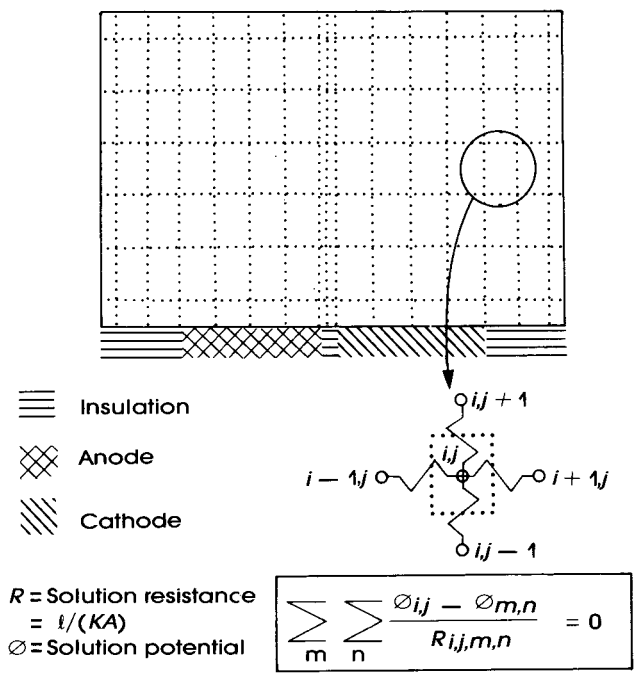

Fig. 2—The essential features of the model

allows it to be used in investigations of the resistance of the metallic conduction path. In this model, the electrochemical boundary conditions are incorporated by the connection of each element adjacent to the surface of the couple to the potential (ϕ_{met}–E_{corr}) through a potential-dependent polarization resistance. ϕ_{met} is the electrostatic potential in the metal substrate on which the electrochemical reaction takes place, and E_{corr} is the open-circuit potential of the electrode of the galvanic couple concerned.

The potential (ϕ_{met}–E_{corr}) is used to account for the relationship between solution potential and interfacial potential, which is expressed by equation (1):

$$E = \phi_{met} - \phi_{soln}, \quad \text{..... (1)}$$

where E = interfacial potential of electrode
ϕ_{met} = electrostatic potential in the metal of the electrode
ϕ_{soln} = electrostatic potential in the electrolyte (adjacent to the electrode).

The effect of the external resistance is simply that the potential in the metal at the anode, ϕ^a_{met}, is less positive than the potential in the metal at the cathode, ϕ^c_{met}, by an amount equal to the current flowing from the cathode to the anode (in the metallic conduction path), multiplied by the external resistance. This relationship is expressed by equation (2):

$$\phi^c_{met} = \phi^a_{met} + I_G R_x, \quad \text{..... (2)}$$

where ϕ^c_{met} = potential in metal at cathode
ϕ^a_{met} = potential in metal at anode
I_G = galvanic current
R_x = resistance of metallic conduction path (external resistance).

This relationship is included in the model in the following way. At the start of each iteration, the total current passing from the anode into the solution is calculated from Ohm's law. (At the conclusion of the calculations when all the potential values have converged, this is, of course, equal to the current arriving at the cathode.) The potential in the metal at the anode is assigned a constant value of 0 V, and the potential in the metal at the cathode is then calculated by use of equation (2).

Comparison of Model Predictions and Experimental Measurements

The experimentally determined polarization diagrams used as model inputs are shown in Fig. 3. The predicted and measured galvanic currents with different resistances in series with the ZRA are plotted in Fig. 4. The diagram shows that the model predictions closely follow the measured values. It is interesting to note that a resistance as large as 10 Ω results in a decrease in the galvanic current of only 1 per cent. This again indicates that the requirement of zero resistance is probably unnecessarily strict, and that the method of measuring the potential drop across a known external resistance to monitor the galvanic current can be valid.

The measured and predicted potential profiles across the couple at a low and a high external resistance are compared in Fig. 5. Again, the model predictions and the experimental measurements are in good accord. It should be mentioned that these diagrams show the potential difference between the conductive substrates of the *anode* and the tin–tin oxide micro-electrode. If the potential difference between the conductive substrates of the *cathode* and the micro-electrode were plotted, the curves would be displaced to more positive potentials by an amount equal to the ohmic potential drop across the external resistance.

Fig. 5 shows the way in which, as the external resistance is increased, the potential profile becomes shallower and moves closer to the open-circuit potential of the anode (which was −0,3 V *vs* Sn/SnO_2). This is due to the fact that the galvanic current decreases, giving a smaller ohmic potential drop (IR-drop) in the solution, as well as resulting in less polarization of the anode. In the limit, with an infinite external resistance (i.e. open-circuit conditions), the potential profile will be a horizontal line at −0,3 V.

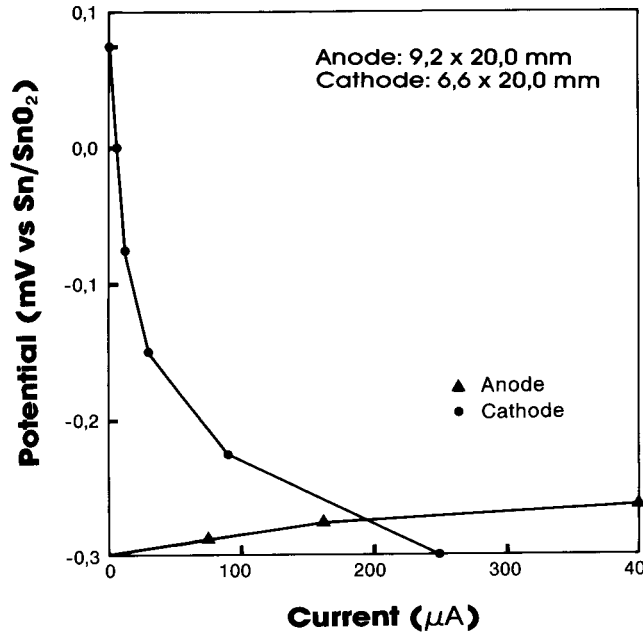

Fig. 3—Anodic and cathodic polarization diagrams of the couple used in the investigation of the influence of external resistance

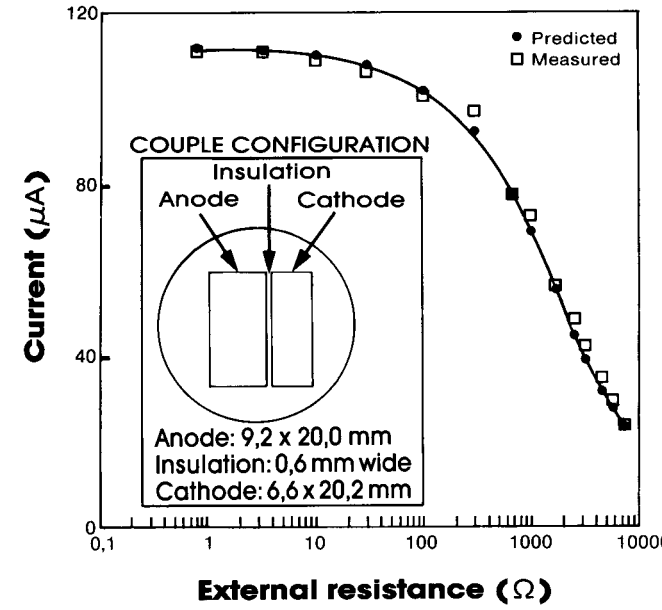

Fig. 4—Predicted and measured short-circuit currents *vs* external resistance (solution conductivity 98,4 mS/m)

These results show that the finite-difference model provides a valid description of this galvanic-corrosion system, including the influence of the resistance of the metallic conduction path.

Effect of External Resistance on the Distribution of the Galvanic Current

The predicted galvanic current densities on the galvanic couple considered here are shown in Fig. 6 for three different values of the external resistance. The diagram demonstrates the way in which the galvanic current is

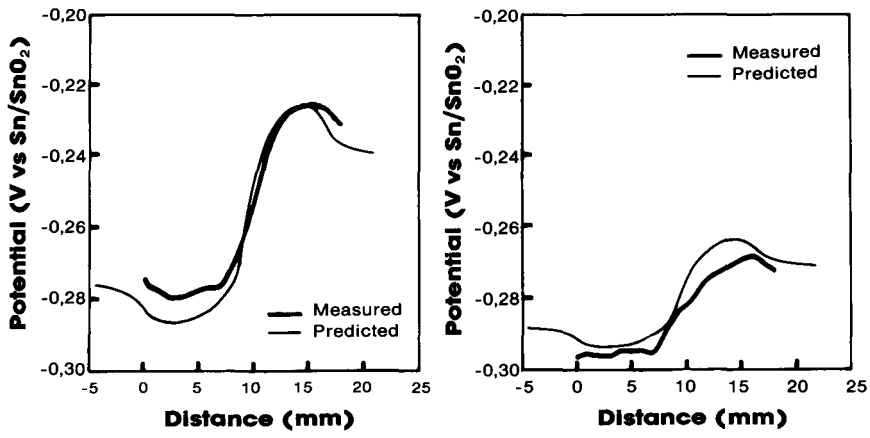

Fig. 5—Comparison of measured and predicted potential profiles at a solution conductivity of 98,4 mS/m (interfacial potential of anode measured)
(a) External resistance 0,762Ω
(b) External resistance 2540Ω

decreased by a higher external resistance. The external resistance also seems to have some effect on the distribution of the galvanic current. The current density appears to become more uniform as the external resistance increases, especially on the cathode. To better illustrate this effect, the current densities given in Fig. 6 are shown in Fig. 7 as relative current densities—each current density is shown relative to the average current density on the anode at that external resistance. This allows better comparison of the *distribution* of the galvanic current, rather than the magnitude of this current.

It is apparent from Fig. 7 that the distribution of the galvanic current is not strongly affected by changes in the external resistance. The main change is on the cathode, where the current density becomes more uniform. This more uniform current density indicates a higher polarization resistance on the cathode. As shown in Fig. 3, the polarization resistance of the cathode does increase as its interfacial potential becomes more positive. Since the effect of the external resistance is to move the interfacial potentials of both electrodes of the couple closer to their open-circuit potentials, this means that, at a higher external resistance, the potential of the cathode is moved into a region of the cathodic polarization diagram, where the polarization resistance is higher. This higher polarization resistance is the cause of the more uniform current distribution on the cathode at the higher values of the external resistance.

Comparison of the Cell Responses to External Resistance

In the macroscopic case that was considered above, there are effectively three resistances to the galvanic current. These are the polarization resistance, the solution resistance, and the external resistance. In the microscopic case, the solution resistance is zero. It is to be expected that, in these two cases, the response of galvanic current to changes in external resistance will be different. In an examination of possible differences, a procedure was developed for the calculation of the effect of external resistance on galvanic current in the microscopic case.

In the microscopic case, the effect of the external resistance can be modelled simply in terms of the IR-drop.

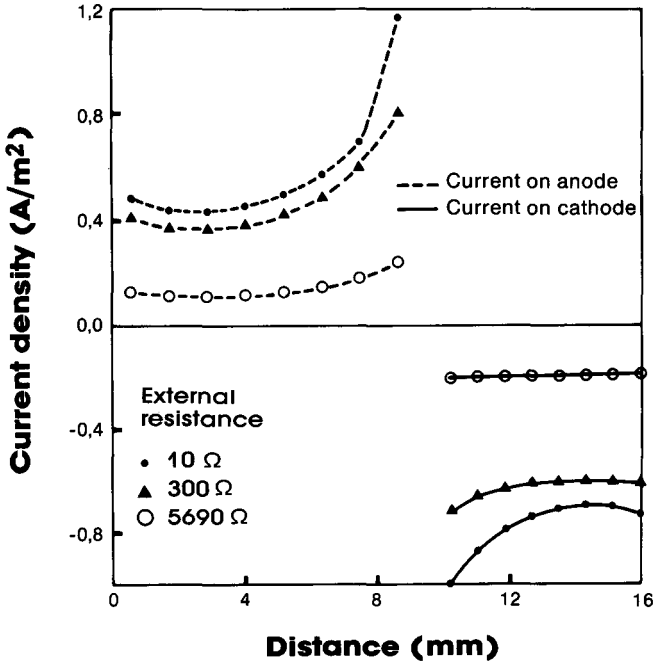

Fig. 6—Influence of external resistance on the distribution of galvanic current as predicted with the finite-difference model (solution conductivity 98,4 mS/m)

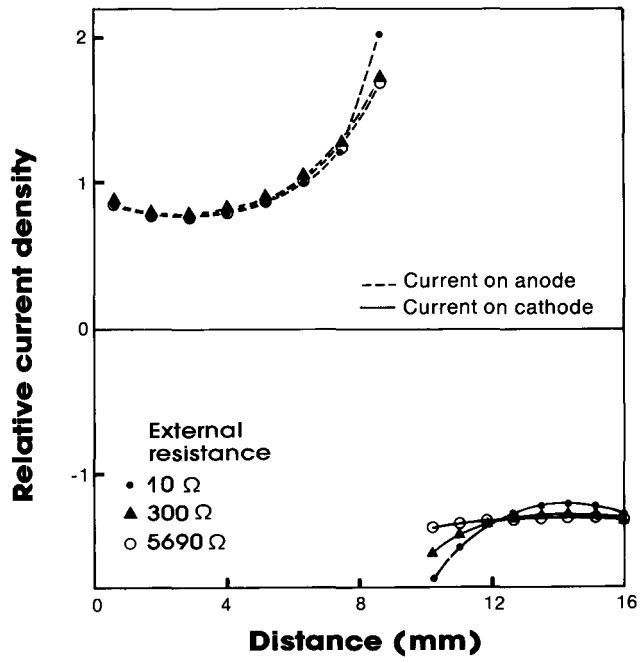

Fig. 7—Relative galvanic-current densities on a couple at different external resistances, expressed relative to the mean density on the anode (solution conductivity 98,4 mS/m)

Across the external resistance, the IR-drop is equal to the difference between the interfacial potentials of the anode and the cathode, and is also equal to the current supplied by the anode and consumed by the cathode at those potentials, multiplied by the external resistance. This defines a unique galvanic current for each value of the external resistance.

The following iterative procedure was used in the calculation of this galvanic current. A first estimate is made of the interfacial potential of the cathode, E_k. The current at that interfacial potential, I, is calculated from the cathodic polarization diagram (the size-dependent polarization diagram that plots *current*, not current density, against potential). The anodic interfacial potential, E_a, which corresponds to this current value is calculated from the anodic polarization diagram. The values of E_k, E_a, and I that satisfy the requirement stated in the paragraph above are denoted by E'_k, E'_a, and I' respectively. The relationship between these is given by

$$E'_k - E'_a = I'R_x. \quad \text{..... (3)}$$

The current I' is related to the current I and the potentials E_k and E'_k, and E_a and E'_a, by the slopes of the cathodic and anodic polarization diagrams (polarization resistances) as described by equations (4a) and (4b):

$$I' = I + (E_k - E'_k)/R^k_p, \quad \text{..... (4a)}$$

$$I' = I + (E'_a - E_a)/R^a_p, \quad \text{..... (4b)}$$

where R^k_p = the mean slope of the curve of E *vs* I for the cathode, between $E = E_k$ and $E = E'_k$

R^a_p = the mean slope of the curve of E *vs* I for the anode, between $E = E_a$ and $E = E'_a$.

When the two expressions for I' given by equations (4a) and (4b) are equated, the following expression for E'_k is obtained:

$$E'_k/R^k_p = E_a/R^a_p + E_k/R^k_p - E'_a/R^a_p. \quad \text{..... (5)}$$

If the value of I is used as an estimate of I' in equation (3), E'_k can be written in terms of E_k, E_a, I, R_x, R^k_p, and R^a_p.

$$E'_k = (E_a + E_k \times R^a_p/R^k_p + IR_x)/(R^a_p/R^k_p + 1). \quad (6)$$

Equation (6) can be used as an iterative formula in the calculation of the galvanic current for different values of the external resistance R_x. From an estimate of E_k, the associated values of E_a and I, and the local slopes of the anodic and cathodic polarization diagrams, a new estimate of E_k, E'_k, is calculated from equation (6). The procedure is repeated until E_k converges. E_k was chosen as the dominant variable in this calculation procedure owing to the smaller dependence of current on potential for the cathode (i.e. a bigger polarization resistance). This should improve the stability of this iterative technique.

The polarization diagrams given in Fig. 3 were used in the calculation of the galvanic current at different values of the external resistance for this microscopic case.

Results and Discussion

The galvanic currents for the macroscopic and microscopic cases are plotted as a function of the external resistance in Fig. 8. The galvanic current is higher in the microscopic case since there it is not limited by the solution resistance, but only by the polarization and external resistances. The curves converge at the higher values of the external resistance since the solution resistance is then much smaller than the external resistance, and the external resistance becomes the main resistance limiting the galvanic current in both cases.

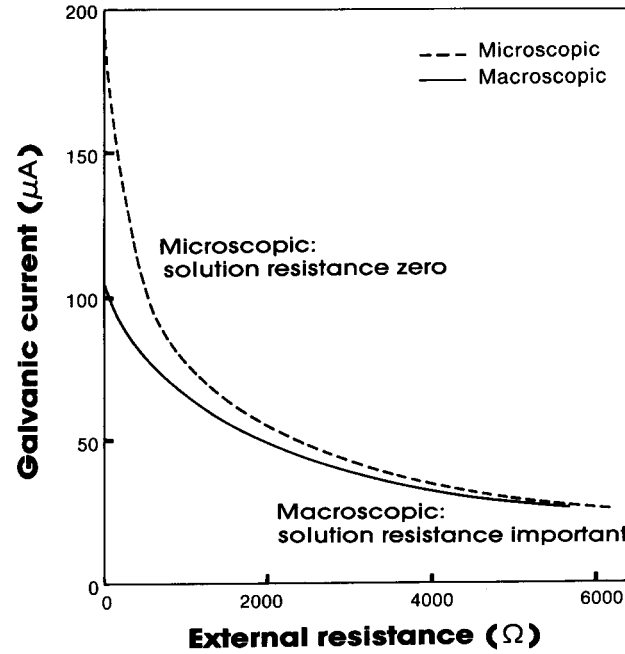

Fig. 8—Responses of microscopic and macroscopic cells to external resistance

It can be seen from Fig. 7 that the actual distribution of the galvanic current was not changed much by a change in the external resistance (in the macroscopic case). The significance of this is that the effective total solution resistance between the anode and the cathode should also be little affected by changes in R_x. The effective total solution resistance is the integral effect of the path length–conduction area combinations along all the current flow paths from the anode to the cathode in the solution. If the distribution of current does not change much, the paths followed by the current will also change little, with the result that the solution resistance is unchanged.

A constant solution resistance will simply add to the external resistance to give the total ohmic resistance that limits the galvanic current. If this were so, the two curves in Fig. 8 would be the same curve, only with an X-axis offset equal to the solution resistance. Fig. 9 shows that this is indeed the case. In Fig. 9, the galvanic currents for the macroscopic and microscopic cases are shown against different X-axes. The X-axis for the macroscopic case is offset relative to the axis for the microscopic case by an amount equal to the solution resistance, which was found to be 478 Ω in this case.

Effect of External Resistance on Galvanic Current

The relationship between the responses of the galvanic current to the external resistance under macroscopic and microscopic conditions, which was established above, suggests that a common practical procedure can be found for the evaluation of the effect of external resistance on

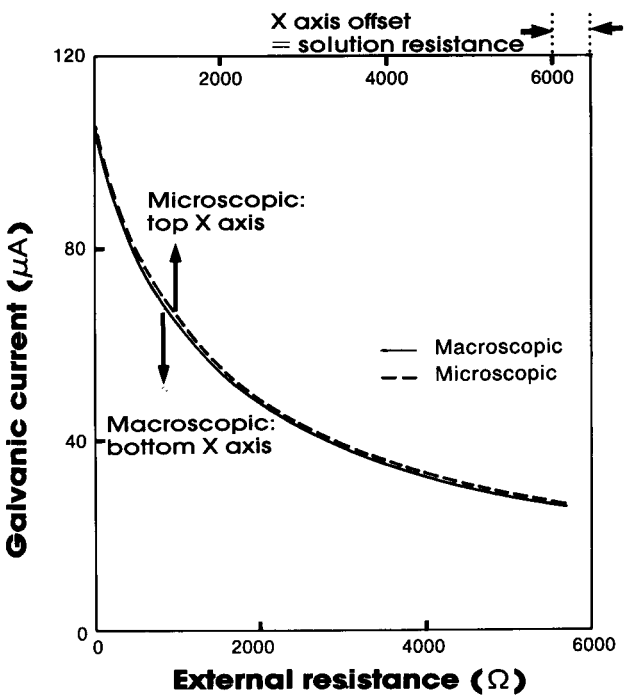

Fig. 9—Solution resistance simply adds to external resistance

galvanic current. Practical evaluation of this effect is important since this will allow an investigator to judge the value of the external resistance that can be tolerated without disturbing the process of galvanic corrosion. When the galvanic current is monitored through measurement of the potential drop across a known resistance, the equipment required is simple. This is an especially attractive method if the galvanic currents of many couples are to be monitored. In that case, the potential drops across the couple resistances can be measured and recorded conveniently by use of a personal computer and multiple inputs of an analogue-to-digital converter.

A simple electrical analogy is used here as the basis of this evaluation procedure. The analogy is that of a potential source of strength, V, connected in series to constant resistances R_p and R_s, and a variable resistance, R_x. The potential V corresponds to the difference between the open-circuit potentials of the electrodes of the galvanic couple, R_p represents the sum of the polarization resistances of the anode and the cathode, R_s represents the solution resistance ($R_s = 0$ in the microscopic case), and R_x is the external resistance. The current in this series circuit when the external resistance is zero is given by

$$I_o = V/(R_p + R_s), \quad \ldots\ldots (7)$$

where I_o = the (galvanic) current when $R_x = 0$.

When the external resistance is not zero, the current is given by equation (8):

$$I = V/(R_p + R_s + R_x), \quad \ldots\ldots (8)$$

where I = the (galvanic) current when $R_x \neq 0$.

The ratio between I_o and I is then equal to

$$I_o/I = 1 + R_x/(R_p + R_s). \quad \ldots\ldots (9)$$

This gives

$$(I_o - I)/I = R_x/(R_p + R_s). \quad \ldots\ldots (10)$$

The fractional decrease in the galvanic current due to the external resistance, $(I_o - I)/I_o$, can be approximated by $(I_o - I)/I$ for small values of R_x, i.e. where I is close to I_o. From equation (10), this means that the fractional decrease in the galvanic current is equal to the ratio of the external resistance to the sum of the polarization resistances and the solution resistance.

To show whether this simple model provides an adequate description of the effect of the external resistance on the galvanic current, the results shown in Fig. 8 are given in Fig. 10 as graphs of the percentage decrease in the galvanic current *vs* the external resistance as a percentage of the sum $(R_s + R_p)$ for percentage decreases in the galvanic current of less than 10 per cent. Hereinafter, this sum of the solution resistance and the polarization resistance will be referred to as the *internal resistance*. For the microscopic case, the internal resistance was calculated simply from the polarization diagrams in Fig. 3. The total internal resistance in this case is the sum of the (size-dependent) polarization resistances of the anode and the cathode. For the macroscopic case, the effective solution resistance of 478 Ω was added to the relevant polarization resistances to give the total internal resistance. These polarization resistances were determined from the polarization diagrams at the galvanic current at zero external resistance.

Fig. 10 shows that this simple analogue can be used to describe the effect of an external resistance on the galvanic current, in both the microscopic and the macroscopic cases. The departure from the 1:1 line at higher relative R_x values is due simply to the substitution of $(I_o - I)/I_o$ for $(I_o - I)/I$, as is shown in Fig. 10.

Fig. 10 suggests a simple procedure for the evaluation of the effect of the external resistance on the galvanic current. The galvanic current with zero external resistance is measured. The resistance value that causes a decrease of, say, 5 per cent in the galvanic current is then determined by the placing of various resistances in series with the ZRA and by monitoring of the galvanic current. Since there is a straight-line dependence of the decrease in the galvanic current on the value of the external resistance, the resistance value determined at a 5 per cent decrease in galvanic current can be interpolated to the acceptable decrease in galvanic current to find the tolerable value of the external resistance. If many galvanic couples are to be monitored, this means that only one ZRA is needed for the initial determination of the acceptable external resistance.

This procedure can be made even more rapid if a potentiostat is used as the ZRA. The potentiostat can be used to impose a potential difference between the cathode and the anode (cathode more positive) in such a way that a 5 per cent decrease in the galvanic current results, relative to the galvanic current with a zero potential difference. The resistance value that this represents can then be calculated from the potential difference imposed and the galvanic current. However, a possible problem with this method can arise from the available accuracy of potential measurement at small overpotentials.

The simple analogy that forms the basis of this pro-

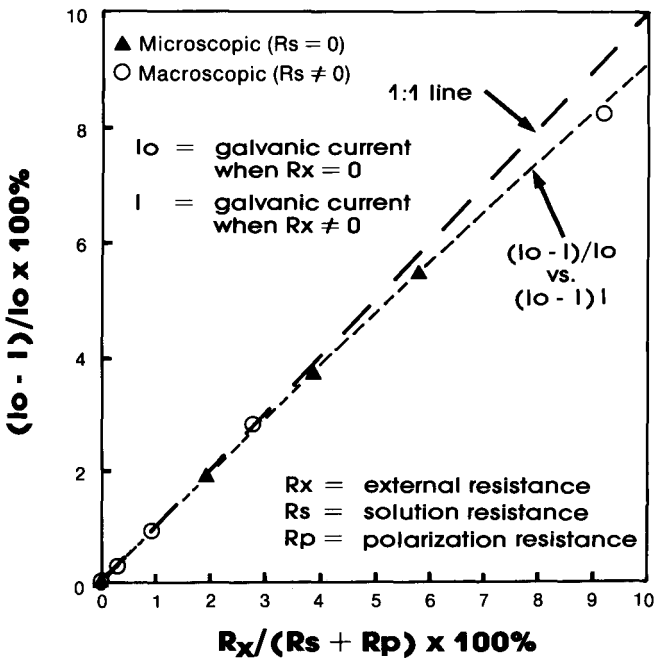

Fig. 10—Decrease in galvanic current *vs* relative external resistance

cedure will be valid if the polarization resistance does not change much with the change in galvanic current (e.g. 5 per cent reduction) used to determine the internal resistance. This is a fair assumption in view of the small change in current considered. For example, a Tafel relationship is assumed between potential and current as follows:

$$\log(I) = \log(I_{corr}) + (E - E_{corr})/\beta, \quad \ldots\ldots\ldots\ldots (11)$$

where I = current
I_{corr} = corrosion current
β = Tafel constant.

The slope of the polarization diagram is then given by

$$dE/dI = \beta/(2{,}303\, I). \quad \ldots\ldots\ldots\ldots (12)$$

From equation (12), a 5 per cent change in the current will result in a change of only (approximately) 5 per cent in the polarization resistance (dE/dI), which shows that the assumption of a constant polarization resistance (when the internal resistance is determined) will probably be justified.

Conclusion

The finite-difference model that was used in the evaluation of the effect of an external resistance on a macroscopic galvanic cell was validated by means of experimental measurements of potential profiles and galvanic currents. The calculation procedure that was developed gives the effect of an external resistance on the galvanic current in a microscopic galvanic cell where the electrodes have polarization diagrams of arbitrary shape. The responses of the galvanic current in microscopic and macroscopic cells to changes in external resistance can be compared by means of this model. From the similarity of these responses, a common method for the practical evaluation of the tolerable external resistance is proposed based on a simple electrical analogy.

Acknowledgements

The authors gratefully acknowledge the financial support provided by Mintek and by Middelburg Steel & Alloys Limited. They also thank Professor G.T. van Rooyen, Head of the Department of Materials Science and Metallurgical Engineering, and Mr Louis Hegyi, both of the University of Pretoria, for their assistance during the construction of the SRET equipment.

References

1. MANSFELD, F., and PARRY, E.P. *Corrosion Sci.*, vol. 12. 1973. p. 605.
2. JONES, D.A. Localized corrosion. *Corrosion science.* Parkins, R.N. (ed.). Applied Science Publishers, 1982. pp. 161–207.
3. ISHIKAWA, Y., HOSAKA, N., and HIOKI, S. Galvanic corrosion testing. *Electrochemical corrosion testing,* ASTM STP 727. Manseld, F., and Bertocci, U. (eds.). American Society for Testing and Materials, 1981. pp. 327–338.
4. HARRIS, B. *Engineering composite materials.* London, The Institute of Metals, 1986. p. 108.
5. TRZASKAMA, P.P. *J. Electrochem. Soc.*, vol. 129, no. 7. 1982. p. 1398.
6. MILLER, R.L., HARTT, W.H., and BROWN, R.P. *Materials Performance,* vol. 15, no. 5. 1976. p. 20.
7. MANSFELD, F. New approaches to atmospheric corrosion research using electrochemical techniques. *Corrosion processes.* Parkins, R.N. (ed.). Applied Science Publishers, 1982. pp. 1–77.
8. FONTANA, M.G., and GREENE, N.D. *Corrosion engineering.* New York, McGraw-Hill, 1967. pp. 205–210.
9. NOWAK, P., KRAUSS, E. and POMIANOWSKI, A. *Hydrometall.*, vol. 12. 1984. p. 95.
10. FONTANA, M.G., and GREENE, N.D. *op cit.*, pp. 28–66.
11. DOIG, P., and EDGINGTON, J.W. *Brit. Corros. J.*, vol. 9, no. 2. 1974. p. 88.
12. ISAACS, H.S., and VYAS, B. Scanning reference electrode techniques in localized corrosion. *Electrochemical corrosion testing,* ASTM STP 727. Mansfeld, F., and Bertocci, U. (eds.). American Society for Testing and Materials, 1981. pp. 3–33.
13. LAUER, G., and MANSFELD, F. *Corrosion,* vol. 26, no. 11. 1970. p. 504.
14. PISTORIUS, P.C., and SANDENBERGH, R.F. To be submitted to *Corrosion Science.*
15. UHLIG, H.H. (ed.). *The corrosion handbook.* New York, John Wiley, 1955. p. 1004.
16. HACK, H.P., and SCULLY, J.R. *Corrosion,* vol. 42, no. 2. 1986. p. 79.
17. TUCK, C.D.S. *Corrosion Sci.*, vol. 30, no. 4. 1983. p. 379.
18. WAGNER, C. *J. Electrochem. Soc.*, vol. 98, no. 3. 1951. p. 116.